# Kyushu University Workshop ”Math-for-Industry Tutorial: Spectral theories of non-Hermitian operators and their application

Stefan LLEWELLYN SMITH

19–20 March 2009

We never linearize, but we do consider the associated linear problem. *Ed Spiegel*

# Chapter 1

# Fluid instability, the continuous spectrum and asymptotic models

## 1.1 Introduction

Fluid flows in the laboratory and in nature present us with many examples of instability. Figure 1.1 shows a small fraction of the range and beauty of instabilities. Fluid dynamicists have been studying instabilities since the 19th century with the work of Reynolds, Rayleigh, Couette and others. In fact the work by Reynolds that led to the very concept of a Reynolds number concerned stability.

The breakdown of apparently simple flows can produce complicated time-dependent structures which are observed in the ocean and atmosphere. For example, the jet stream, the Gulf Stream (see Figure 1.1), the wake behind Jan Mayen island and other features can be interpreted as the result of the instability of a jet-like flow. In the geophysical context, it is interesting to understand why the entire flow structure, perturbed though it may be from some putative underlying simple jet or other basic state, does not break down completely into turbulence. The stratification and rotation present in large-scale geophysical flows play an important role in this persistence of coherent structures. We shall not investigate these physical effects, but we will look at coherent structures.

In many applications, one seeks to minimize instabilities so as to retain a certain laminar flow over a range of parameters, or instead to maximize instabilities and hence obtain a turbulent flow (e.g. to enhance mixing). We will not discuss the transition to turbulence at all here.

### 1.1.1 Stability and instability

Reynolds' original experimental apparatus still survives. As is well known, he examined the nature of flow in a smooth pipe as he increased the flow rate. In modern terms, he was increasing the Reynolds number. What he found was that the laminar (literally 'sheet-like', i.e. smooth.) state of motion was replaced by a complex turbulent motion that eventually filled the width of the pipe and led to efficient mixing. Figure 1.2 shows a typical experimental result.

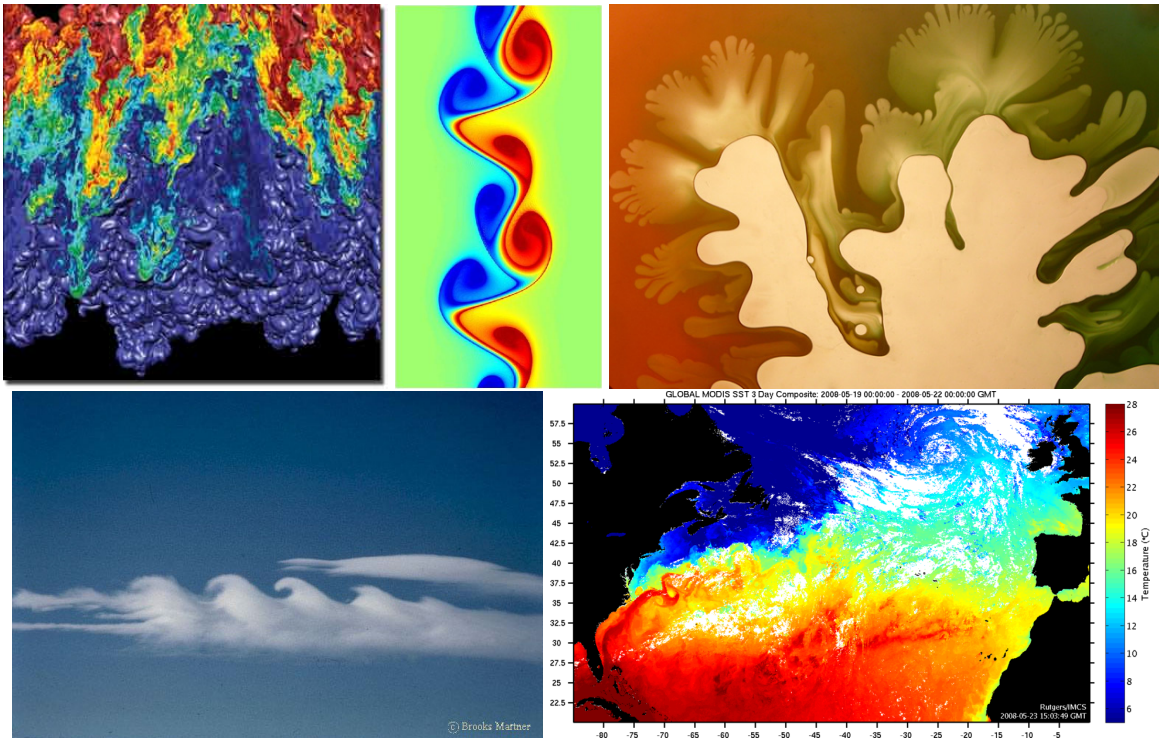


Figure 1.1: From left to right and top to bottom. Rayleigh–Taylor instability, simulated on the Blue Gene supercomputer. Shear instability of a jet: meanders formed on the jet have broken up to form vortices. Saffman–Taylor instability. Kelvin–Helmholtz instability visualized by clouds. Gulf Stream eddies visualized by SST (Sea Surface Temperature). References are at the of the chapter.

As it happens, the particular problem of the stability of pipe flow is a difficult one and not yet fully understood (cf. e.g Willis *et al.* 2008). However, the idea that the flow is laminar for a control parameter (here the Reynolds number) below some critical value and unstable above it is fundamental to the whole field. The experimental protocol of changing the Reynolds number and observing the response of the fluid corresponds to the theoretical problem of understanding the stability of the flow at a given value of the Reynolds number (or other control parameter). The notion of a critical value of a control parameter $R$ requires a little discussion, and one is given in Schmid & Henningson (2001). This is related to the various notions of stability that exist in the dynamical systems literature (e.g. Lyapunov stability, asymptotic stability,...). For now we shall limit ourselves to the critical value obtained from the linear stability problem. As it happens we shall often be working in the inviscid case where there is no control parameter, and the flow is either unstable or not, depending on its velocity profile.

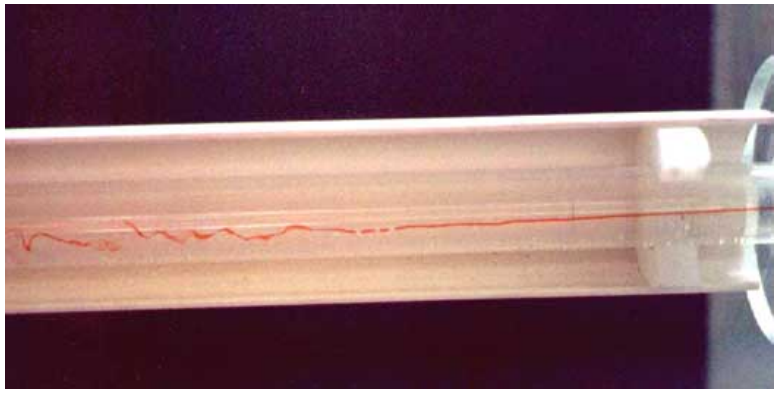

Figure 1.2: Transition from laminar to turbulent flow in pipe (Reynolds' experiment). The laminar flow entering the pipe from the right breaks up and becomes disordered.

### 1.1.2 Outline

In this lecture, I will give a quick overview of what might be called the classical theory of fluid stability. My goal is to proceed rapidly through the basics to reach critical layers and the continuous spectrum. These will motivate an outline of more recent work on 'vorticity defects'. This defect theory is drawn from the work of del-Castillo-Negrete, Balmforth & Young (1999), in which further details can be found.

I feel quite apprehensive about providing such an overview, given the wealth of excellent books and articles available (as well as the prospect of following Sherwin Maslowe). I have drawn heavily from the following sources: Lin (1966), Drazin & Reid (1981), Maslowe (1985), Drazin (2002a) and Schmid & Henningson (2001). Other relevant books include Chandrasekhar (1961), Betchov & Criminale (1967), Joseph (1967) and Criminale, Jackson & Joslin (2003). I will not begin to list the many relevant articles. Any shortness of treatment can be remedied from these sources.

## 1.2 Classical theory

### 1.2.1 Preliminaries

We limit ourselves to flows with constant density and without free surfaces, moving boundaries, background rotation, magnetic fields or other effects. We are hence losing a host of physical mechanisms that can destabilize or stabilize a flow. The only parameters remaining in our problem are viscosity and the background flow and geometry of the system. If we non-dimensionalize our equations with an appropriate velocity scale $U$ and length scale $L$, we are solving the Navier–Stokes equations

$$\frac{\mathrm{D}\mathbf{u}}{\mathrm{D}t} = -\nabla p + \frac{1}{Re}\nabla^2\mathbf{u}, \tag{1.1}$$

$$\nabla\cdot\mathbf{u} = 0, \tag{1.2}$$

where $\mathbf{u}$ and $p$ are the dimensionless velocity and pressure, and $Re \equiv UL/\nu$ is the Reynolds number, with $\nu$ the kinematic viscosity. The appropriate no-slip boundary condition is then $\mathbf{u} = \mathbf{0}$. In what follows we will also consider the inviscid case where $Re \to \infty$. In that case we lose the highest derivative and the boundary condition applied to the normal velocity component, giving $\mathbf{u}\cdot\mathbf{n} = 0$, the no-penetration condition. If the flow domain is unbounded, some sort of decay or boundedness condition on velocity is required. This is usually fairly clear.

The fundamental idea is that we have some basic state, i.e. a velocity field $\mathbf{U}$ and a pressure field $P$. We wish to understand if, given some initial perturbation, the perturbation grows. In the linearized approach, we neglect quadratic quantities in the governing equations. Then the linearized equations for the perturbation ($\mathbf{u}'$, $p'$) become

$$\frac{\partial \mathbf{u}'}{\partial t} + \mathbf{U}\cdot\nabla\mathbf{u}' + \mathbf{u}'\cdot\nabla\mathbf{U} = -\nabla p' + \frac{1}{Re}\nabla^2 p', \tag{1.3}$$

$$\nabla\cdot\mathbf{u}' = 0. \tag{1.4}$$

The coefficients of this equation are independent of time, so one can find normal mode solutions with $\mathrm{e}^{\sigma t}$ dependence. Similarly, if $\mathbf{U}$ is independent of $y$, one can write the solution (or Fourier transform) as being proportional to $\mathrm{e}^{\mathrm{i}\beta y}$.

What basic states are possible? The classical geometry is unidirectional flow in a channel so that $\mathbf{U} = U(z)\mathbf{i}$. Then, depending on the boundary conditions, the basic state is a combination of Couette and plane Poiseuille flow. One can consider semi-infinite domains in which one can obtain e.g. boundary-layer profiles such as the Blasius boundary layer. Formally this is problematic. Not so much because the equations are not satisfied (one could add a body force to fix this – see e.g. Young & Manfroi 2002 and other work on Kolmogorov flows), but rather because of non-parallelism. One can argue that these flows vary slowly in the alongstream direction and are hence *nearly parallel*, but this does not resolve the fundamental problem. I will skirt over these problems for now. If one moves to the inviscid case, any profile $U(z)$ is possible, both in channels and in unbounded geometries. Flow with azimuthal symmetry, i.e. $\mathbf{u} = u(r)\mathbf{e}_\theta$ has similar properties: Couette flow in the viscous case, anything in the inviscid case.

### 1.2.2 The Orr–Sommerfeld equation

This is the name applied to the equation governing disturbances to Couette and Poiseuille flow (and more generally to nearly parallel flows but see above). We start from the disturbance equations written in terms of $\mathbf{u}' = (\hat{u}, \hat{v}, \hat{w})\mathrm{e}^{\mathrm{i}\alpha(x-ct)+\mathrm{i}\beta y}$. Here $\sigma = -\mathrm{i}\alpha c$ so the imaginary part of $c$ determines the stability of the flow. The disturbance equations are

$$\{\mathrm{D}^2 - (\alpha^2+\beta^2)^2 - \mathrm{i}\alpha Re(U-c)\}\hat{u} = ReU'\hat{w} + \mathrm{i}\alpha Re\hat{p}, \tag{1.5}$$

$$\{\mathrm{D}^2 - (\alpha^2+\beta^2)^2 - \mathrm{i}\alpha Re(U-c)\}\hat{v} = \mathrm{i}\beta Re\hat{p}, \tag{1.6}$$

$$\{\mathrm{D}^2 - (\alpha^2+\beta^2)^2 - \mathrm{i}\alpha Re(U-c)\}\hat{w} = Re\mathrm{D}\hat{p}, \tag{1.7}$$

$$\mathrm{i}(\alpha\hat{u} + \beta\hat{v}) + \mathrm{D}\hat{w} = 0 \tag{1.8}$$

where $\mathrm{D} = \mathrm{d}/\mathrm{d}z$. At rigid boundaries we have $\hat{u} = \hat{v} = \hat{w} = 0$.

We can immediately simplify our life by invoking Squire's transformation. Write

$$\tilde{\alpha} = (\alpha^2 + \beta^2)^{1/2}, \quad \tilde{\alpha}\tilde{u} = \alpha\hat{u} + \beta\hat{v}, \quad \frac{\tilde{p}}{\tilde{\alpha}} = \frac{\hat{p}}{\alpha}, \quad \tilde{w} = \hat{w}, \quad \tilde{c} = c, \quad \tilde{\alpha}\tilde{Re} = \alpha Re. \tag{1.9}$$

Then we find

$$\begin{aligned} \{\mathrm{D}^2 - \tilde{\alpha}^2 - \mathrm{i}\tilde{\alpha}\tilde{Re}y(U-c)\}\tilde{u} &= ReU'\tilde{w} + \mathrm{i}\tilde{\alpha}\tilde{Re}\tilde{p}, & (1.10)\\ \{\mathrm{D}^2 - \tilde{\alpha}^2 - \mathrm{i}\tilde{\alpha}\tilde{Re}y(U-c)\}\tilde{w} &= \tilde{Re}\mathrm{D}\tilde{p}, & (1.11)\\ \mathrm{i}\tilde{\alpha}\tilde{u} + \mathrm{D}\tilde{w} &= 0. & (1.12) \end{aligned}$$

But these are the same equations as in the two-dimensional case. Since $\tilde{\alpha} \geq \alpha$, we obtain $\tilde{Re} \leq R$ and *Squire's theorem*: it is sufficient to consider two-dimensional disturbances to obtain the minimum critical Reynolds number.

Since we are now working in two dimensions we can consider the evolution of the amplitude of the streamfunction, $\phi(z)$. We can obtain a single equation either by manipulating the above equations or by considering the vorticity equation. The result is the Orr–Sommerfeld equation

$$(\mathrm{i}\alpha Re)^{-1}(\mathrm{D}^2 - \alpha^2)^2\phi = (U-c)(\mathrm{D}^2 - \alpha^2)\phi - U''\phi, \tag{1.13}$$

with boundary conditions $\phi = \mathrm{D}\phi = 0$ at the boundaries. This equation may be solved to given an eigenvalue relation of the form

$$\mathcal{F}(\alpha, c, Re) = 0. \tag{1.14}$$

For bounded flows and analytic $U(z)$, the eigenvalue spectrum is discrete (Lin 1961). For unbounded flows, the spectrum e.g. of the Blasius boundary layer consists of a finite number of discrete eigenvalues and a continuous spectrum for which the eigenfunctions oscillate sinusoidally for large $z$.

The Orr–Sommerfeld equation is of fourth order. This may seem paradoxical since the original set of equations is sixth order. Squire's transformation has decreased the order of the system by two. In fact there is an associated decoupled equation in addition to (1.13), known as Squire's equation, whose solutions are stable. However Squire's equation may be relevant for transient growth situations. For more complicated geometry, this decoupling need not occur (e.g. Drazin 2002 § 8.10).

The effect of viscosity can be destabilizing as well as stabilizing. The former is perhaps unexpected. A great deal of work has been carried out on the Orr–Sommerfeld equation, in particular to understand the behavior of the neutral curve $c_i = 0$ for large $Re$. This work is complicated and would take us too far afield. Instead we move to the inviscid case on our way to defect theory.

### 1.2.3 The Rayleigh equation

Formally we take $Re = \infty$. An inviscid version of Squire's transformation still holds and we obtain Rayleigh's equation for the streamfunction $\phi$:

$$(U-c)(\mathrm{D}^2 - \alpha^2)\phi - U''\phi = 0, \tag{1.15}$$

with boundary condition $\phi = 0$ at the boundaries (or decay in unbounded domains).

A number of important results about $c$ can be obtained from (1.15) associated with the names of distinguished mathematicians and physicists. Assume $c_i > 0$ and multiply (1.15) by $\phi^*$, integrate over the domain $(z_1, z_2)$, integrate by parts and use the boundary conditions. Then

$$\int_{z_1}^{z_2} (|\phi'|^2 + \alpha^2|\phi|^2)\,\mathrm{d}z + \int_{z_1}^{z_2} \frac{U''}{U-c}|\phi|^2\,\mathrm{d}z = 0. \tag{1.16}$$

The imaginary part is

$$c_i \int_{z_1}^{z_2} \frac{U''}{|U-c|^2}|\phi|^2\,\mathrm{d}z = 0 \tag{1.17}$$

and for an unstable mode with $c_i > 0$, $U''$ must change sign in the interval $(z_1, z_2)$. This is *Rayleigh's criterion*, a necessary condition for instability that can be used to show that certain flows are stable. Fjørtoft obtained a stronger form: a necessary condition for instability is that $U''(U - U_s) < 0$ somewhere in the flow, where $z_s$ is a point at which $U''(z_s) = 0$ and $U(z_s) = U_s$. Finally Howard showed that if a mode is unstable, then

$$[c_r - \tfrac{1}{2}(U_m + U_M)]^2 + c_i^2 \leq [\tfrac{1}{2}(U_M - u_m)]^2. \tag{1.18}$$

This is the *Howard semicircle theorem* and shows that the $c$ lies in a semicircle in the upper half-plane.

It is usual at this point to go through examples using broken line profiles, for which analytic results can be obtained, but we move on.

### 1.2.4 Neutral modes and critical layers

Rayleigh's equation (1.15) has a singularity at points in the domain where $U(z_c) = c$ if $U_m \leq c \leq U_M$. These $z$-values are known as critical levels or layers. This property was termed by Kelvin (1880) 'The disturbing infinity in Lord Rayleigh's solution'. The nature of the streamlines near the critical point was found by Kelvin (1880). Since the mode is neutral, one can carry out a Galilean transformation so that the velocity profile is $U(z) - c$. Then the equation of streamlines become approximately

$$\tfrac{1}{2}U'(z_c)(z - z_c)^2 + A\phi(z_c)\cos\alpha x = \text{constant}. \tag{1.19}$$

This is the famous cat's eye pattern, shown in Figure 1.3. Note that if the velocity gradient vanishes at the critical point, this picture no longer holds. The behavior of such flows can be rather different.

In fact there are two families of eigensolutions for smooth $U$. First a discrete spectrum of complex conjugate pairs $c$ and $c^*$; the number of pairs is less or equal than the number of inflection points of $U$ (so there may be none). Second a continuous spectrum for all $c$ in the range $[U_m, U_M]$ with eigenfunctions that have a discontinuous derivative at $z_c$.

All neutral modes that are the limit of unstable modes as $c_i \to 0$ have critical points, although they are not necessarily singular since $U - c$ can vanish at the critical points. While $c$ and $c^*$ are both eigenvalues of the same Rayleigh equation, the unstable mode of the two has a clear relation with the O–S problem, while the damped mode in general does not.

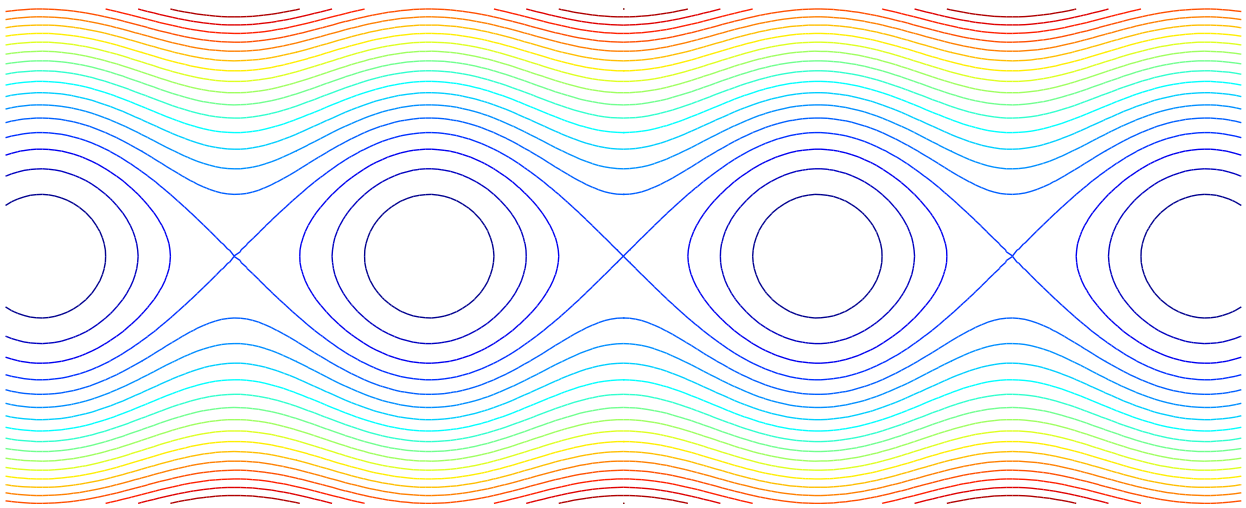

Figure 1.3: Cat's eye pattern.

### 1.2.5 The continuous spectrum

An analysis of the Rayleigh equation near critical points can be carried out using Frobenius series. One solution has a logarithmic singularity. The correct choice of path in the complex plane to avoid this singularity has to be determined using extra information. The obvious way is from the viscous theory. An alternative approach is to consider the inviscid initial-value problem. The very existence of situations with no discrete modes shows that the continuous spectrum is required to solve the initial-value problem for the inviscid problem (the discrete modes of the O–S equation form a complete set for bounded domains however).

The case of Couette flow is the canonical example. The base profile is $U = z$ between $z = -1$ and $z = 1$. Then the underlying linearized equation becomes

$$\left(\frac{\partial}{\partial t} + z\frac{\partial}{\partial x}\right)\nabla^2\psi = 0.$$

This has no discrete modes. Orr (1907) proceeded by solving

$$\nabla^2\psi = F(x - zt, z)$$

as a Fourier series in $z$. A more general approach was developed by Eliassen, Høiland & Riis (1953), Case (1960) and Dikii (1960). One Fourier transforms (1.2.5) in space and Laplace transforms in time. Another approach is to use generalized functions: the Rayleigh equation is

$$(z - c)(\mathrm{D}^2 - \alpha^2)\phi = 0, \qquad \phi(-1) = \phi(1) = 0,$$

from which one obtains not just

$$(\mathrm{D}^2 - \alpha^2)\phi = 0,$$

the equation for the discrete modes with no solutions, but also

$$(\mathrm{D}^2 - \alpha^2)\phi = \delta(z - c),$$

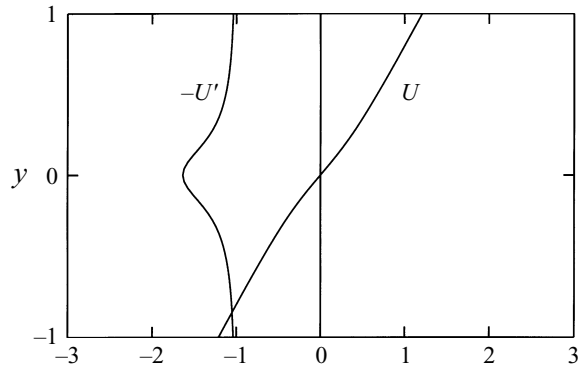


Figure 1.4: Couette flow with superimposed vorticity effect. From Balmforth, del-Castillo-Negrete & Young (1997).

which gives the continuous spectrum. A full solution of the system is then easily found in closed from (in the Laplace variable). For general flows, the same procedure works formally. The resulting decay for streamfunction and vorticity led to some contention. Fro an initial disturbance occupying a finite domain in $x$, the correct result is $\psi = O(t^{-2})$, whereas earlier attempts had found $\psi = O(t^{-1})$. As pointed out by Maslowe (1981), the initial-value approach and the inviscid limit of the O–S equation are not formally equivalent. The former breaks down for large times near critical levels.

## 1.3 Defects in shear

### 1.3.1 Motivation

We consider a shear flow inside which there is embedded a region in which vorticity varies rapidly – see Figure 1.4 for an illustration of the situation. This rapid variation is viewed as a defect atop the background ambient shear. Previously versions of this approach had been developed for Couette flow by Gill (1965) and Lerner & Knobloch (1988) in the linear and inviscid cases respectively. These works showed that the defect could destabilize the Couette flow. The current matched asymptotic expansion framework is related to the approach used by Stewartson (1978) and others to study forced Rossby critical wave layers. For purely inviscid disturbances, we are led to an approximate description that bears some similarity to the Vlasov equation of plasma physics. We work with Couette flow here, but the ideas generalize to arbitrary background flows.

### 1.3.2 Derivation

The non-dimensional equation of motion for the disturbance streamfunction $\psi$ is the two-dimensional vorticity equation. The background flow is sustained by a forcing term $F(y/\epsilon)$, where $\epsilon$ measures the size of the defect region as well as the size of the disturbance with respect to the basic state. If $F = 0$, the basic state is Couette flow (which

needs no forcing). Then

$$\epsilon\nabla^2\psi_t + y\nabla^2\psi_x + \epsilon^2\frac{\partial(\psi,\nabla^2\psi)}{\partial(x,y)} = \epsilon\alpha(\epsilon^{-1}F - \nabla^2\psi) - \epsilon^3\nu\nabla^2(\epsilon^{-1}F - \nabla^2\psi). \tag{1.20}$$

The disturbance velocity is $(u,v) = (-\psi_y, \psi_x)$, the 'geophysical convention'. Ekman friction (a scale-free damping that appears naturally in geophysical problems) is included, with time-scale $\alpha^{-1}$. Viscosity is also retained, with coefficient $\nu$. The domain is $-1 < y < 1$ with boundary conditions $\psi(x,\pm 1,t) = 0$.

Expanding $\psi$ in $\epsilon$, we obtain

$$y\nabla^2\psi_0 = 0. \tag{1.21}$$

We allow for action near $y = 0$, so the appropriate equation, which corresponds physically to vorticity begin confined near the region, is

$$\nabla^2\psi_0 = -2A(x,t)\delta(y). \tag{1.22}$$

This is reminiscent of (1.2.5). We solve using Fourier transforms defined by

$$\tilde{\psi}_0(k,y,t) \equiv \int_{-\infty}^{\infty} \psi_0(x,y,t)\mathrm{e}^{\mathrm{i}kx}\,\mathrm{d}x \tag{1.23}$$

and obtain

$$\tilde{\psi}(k,y,t) = \tilde{A}(k,t)k^{-1}\operatorname{sech} k \sinh\left[k(1-|y|)\right] = \tilde{B}(k,t)\operatorname{cosech} k \sinh\left[k(1-|y|)\right], \tag{1.24}$$

where $B(x,t) \equiv \psi(x,0,t)$. The transforms of the functions $A$ and $B$ are related by

$$\tilde{B}(k,t) = k^{-1}\tanh k\tilde{A}(k,t). \tag{1.25}$$

To quote BdCNY, 'the outer flow is driven by the defect, which introduces the term $-2A(x,t)\delta(y)$. This source induces an irrotational outer flow which in turn advects the defect. This advection is associated with the streamfunction at the defect, denoted by $B(x,t)$. The system is closed by examining the inner region in which $y = O(\epsilon)$.'

Inside the defect we define an inner variable $\eta \equiv y/\epsilon$. Then, by writing

$$\psi = B(x,t) + \epsilon\varphi_1(x,\eta,t) + O(\epsilon^2), \tag{1.26}$$

we obtain the matching condition

$$2A(x,t) = -\int_{-\infty}^{\infty} Z(x,\eta,t)\,\mathrm{d}\eta. \tag{1.27}$$

where $Z(x,\eta,t) = \varphi_{1\eta\eta}$ is the (scaled) vorticity in the defect. Substituting into (1.20) leads to the system

$$Z_t + \eta Z_x + B_x Z_\eta = \alpha(F - Z) - \nu(F - Z)_{\eta\eta}, \tag{1.28}$$

$$2\tilde{B}(k,t) = -k^{-1}\tanh k\int_{-\infty}^{\infty}\tilde{Z}(k,\eta,t)\,\mathrm{d}\eta. \tag{1.29}$$

This is the equation set we shall consider from now on.

When the dissipative terms are set to zero, (1.29) becomes analogous to the Vlasov equation of plasma physics (see the appendix below). In this analogy, $\eta$ is a velocity-like coordinate, the defect vorticity, $Z(x,\eta,t)$, plays the role of particle distribution function, and $B(x,t)$ corresponds to the potential of the electric field. Unlike the Vlasov problem, the vorticity can have either sign.

### 1.3.3 Inviscid stability results

We can now return to the linear stability problem for smooth profiles and nevertheless obtain analytic results. Consider flows in which $Z$ and $B$ are independent of $x$, i.e.

$$Z(x,\eta,t) = F(\eta) + \zeta, \qquad B(x,t) = \frac{1}{2}\int_{\infty}^{\infty} F(\eta')\,\mathrm{d}\eta' + b(x,t). \tag{1.30}$$

Then neglecting the nonlinear term and dissipative effects gives the associated linear problem

$$\zeta_t + \eta\zeta_x + b_x F_\eta = 0, \qquad 2\tilde{b}(k,t) = -k^{-1}\tanh k \int_{\infty}^{\infty} \tilde{\zeta}(k,\eta,t)\,\mathrm{d}\eta. \tag{1.31}$$

For now we seek modal solutions proportional to $\mathrm{e}^{\mathrm{i}(kx-\omega t)}$. Substituting and integrating over $\eta$ gives the dispersion relation

$$\int_{-\infty}^{\infty} \frac{F_\eta(\eta)}{\eta - c}\,\mathrm{d}\eta = 2k\coth k, \tag{1.32}$$

a relation first found by Gill (1965). Analogues of the Rayleigh and Fjørtoft theorems can also be derived (the former is not terribly useful).

### 1.3.4 Nyquist theory

It is possible to do better than the necessary conditions derived so far to obtain a qualitatively complete understanding of the modal stability problem. The dispersion relation (1.32) can be written as

$$D(c,k) \equiv 2k\coth k - \int_{-\infty}^{\infty} \frac{F_\eta(\eta)}{\eta - c}\,\mathrm{d}\eta, \tag{1.33}$$

and instability corresponds to zeros of function $D$ in the upper half plane. The function $D$ is analytic in the $c$-plane except along the $c_r$-axis where it has a branch cut. The number of zeros in the upper half-plane is then equal to the number of times $\gamma'$, the image of the semicircle $\gamma$ with infinite radius in the upper half-plane, encircles the origin in the $D$-plane.

### 1.3.5 The initial-value problem

The discrete spectrum is not complete. As above, we can study the initial-value problem using Laplace transform techniques. The results show the various effects of transient amplification of the continuum, its eventual decay, and the sustained growth of unstable normal modes.

For Couette flow with $F = 0$, the Kelvin–Orr solution $\zeta(x,\eta,t) = \zeta_0(x - \eta t, \eta)$ leads to an explicit integral for $\tilde{b}(k,t)$. One can manufacture qualitatively different examples of growth followed by decay. There is no universal expression for the time dependence

of the streamfunction, but provided the initial condition is infinitely differentiable in $\eta$, $b(x,t)$ vanishes faster than any power of $t$ as $t \to \infty$. This result differs from the well-known result that the streamfunction of a perturbation to a stable shear flow decays as $t^{-2}$. This contradiction is resolved at the next order in the expansion of the streamfunction within the defect: $\varphi_1(x,\eta,t)$ exhibits the universal asymptotic decay $t^{-2}$.

For the case with non-zero $F(\eta)$ we use a Fourier-Laplace transform. The result is

$$\tilde{b}(k,t) = \frac{1}{2\pi \mathrm{i}} \int_{p_0-\mathrm{i}\infty}^{p_0+\mathrm{i}\infty} \frac{N}{D} \mathrm{e}^{pt} \, \mathrm{d}p, \tag{1.34}$$

where the integration contour lies to right of the abscissa of convergence. We have seen the function $D$ before. The function $N$ is similar. The behavior of (1.34) is governed by its singularities. Zeros of $D$ with $p_r > 0$ correspond to unstable normal modes. Modes with $p_r < 0$ however are not stable normal modes, but are zeros of the analytical continuation of $D$. They are 'Landau poles' and contribute exponentially decaying responses to $b(x,t)$. There can also be singularities of $N$; these do not appear to have a name.

### 1.3.6 The viscous problem

Restoring the viscous and dissipative terms gives

$$\zeta_t + \eta\zeta_x + b_x F_\eta = -\alpha\zeta + \nu\zeta_{\eta\eta}, \qquad 2\tilde{b}(k,t) = -k^{-1} \tanh k \int_{\infty}^{\infty} \tilde{\zeta}(k,\eta,t) \, \mathrm{d}\eta. \tag{1.35}$$

Ekman damping just shifts the imaginary part of the normal modes. Diffusion is a singular perturbation. We can obtain the analog of the O–S equation and apply to it the Nyquist procedure.

## 1.4 Conclusion

I have presented classical results of stability theory and a theory for the evolution of a small, localized vorticity defect. The resulting equation has a simplified nonlinear term similar of the Vlasov equation. It is straightforward to obtain a number of explicit results, including dispersion relations, a Nyquist method, and the initial-value problem.

Further developments include more investigation of the viscous case (Balmforth 1998) and an axisymmetric version (see Lecture 2). Two other possibilities have not been investigated to my knowledge. One is the case where the ambient shear is non-monotonic: there is then the possibility of multiple defects that interact with one another and analysis then gives coupled Vlasov-like equations for the defects. The second is the case of defects located near the points of vanishing shear (e.g. Brunet & Haynes 1995).

# Appendix: the Vlasov equation

The Vlasov equation describes the dynamics of a plasma made up of particles with a long-range force. The dependent variables are $f_e(\mathbf{x},\mathbf{p},t)$ and $f_i(\mathbf{x},\mathbf{p},t)$, the electron and

ion distribution functions, that depend on position $\mathbf{x}$, momentum $\mathbf{p}$ and time $t$. The governing equations for the distribution $f_\alpha$ is

$$\frac{\partial f_\alpha}{\partial t} + \mathbf{u}\cdot\frac{\partial f_\alpha}{\partial \mathbf{x}} + \frac{q_\alpha \mathbf{E}}{m_\alpha}\cdot\frac{\partial f_\alpha}{\partial \mathbf{p}} = 0, \tag{1.36}$$

where the notation emphasizes that $f$ depends both on $\mathbf{x}$ and $\mathbf{p}$. The charge and mass of species $\alpha$ are $q_\alpha$ and $m_\alpha$ respectively. The electric field satisfies a Poisson equation:

$$\nabla\cdot\mathbf{E} = 4\pi\rho, \tag{1.37}$$

where $\rho$ is the charge density given by

$$\rho = e\int (f_e - f_i)\mathrm{d}\mathbf{p}. \tag{1.38}$$

Notice the similarity to the Boltzmann equation. In fluid descriptions of plasmas, one integrates away the momentum dependence.

## 1.5 References

### Books


Betchov, R. & Criminale, W. O., Jr. (1967) *Stability of Parallel Flows* Academic Press, New York.

Chandrasekhar, S. (1961) *Hydrodynamic and Hydromagnetic Stability* Dover, New York.

Criminale, W. O., Jackson, T. L. & Joslin, R. D. (2003) *Theory and Computation in Hydrodynamic Stability* Cambridge University Press, Cambridge.

Drazin, P. G. (2002) *Introduction to Hydrodynamic Stability* Cambridge University Press, Cambridge.

Drazin, P. G. & Reid, W. H. (1981) *Hydrodynamic stability* Cambridge University Press, Cambridge.

Joseph, D. D. (1976) *Stability of fluid motions* Springer, Berlin.

Lin, C. C. (1966) *The theory of hydrodynamic stability* Cambridge University Press, Cambridge.

Schmid, P. J. & Henningson, D. S. (2001) *Stability and Transition in Shear Flows* Springer, New York.


### Articles


Balmforth, N. J. (1998) Stability of vorticity defects in viscous shear. *J. Fluid Mech.* **357** 199–224.

Balmforth, N. J., del-Castillo-Negrete, D. & Young, W. R. (1997) Dynamics of vorticity defects in shear. *J. Fluid Mech.* **333** 197–230.

Brunet, G. & Haynes , P. H. (1995) The nonlinear evolution of disturbances to a parabolic jet. *J. Atmos. Sci.* **52** 464–477.

Case, K. (1960) Stability of inviscid Couette flow. *Phys. Fluids* **3** 143–148.
Dikii, L. A. (1960) On the stability of plane parallel flows of an inhomogeneous fluid. *Prikl. Mat. Mekh.* **24** 249–259. Translated in *J. Appl. Math. Mech.* **24** 257–369.
Eliassen, A., Høiland, E. & Riis, E. (1953) Two-dimensional perturbations of a flow with constant shear of a stratified fluid. *Instl. Weather Climate Res. Oslo,* Publ. No. 1.
Gill, A. E. (1965) A mechanism for instability of plane Couette flow and of Poiseuille flow in a pipe. *J. Fluid Mech.* **21**, 503–511.
Kelvin, Lord (1880) On the vibrations of a columnar vortex. *Phil. Mag.* **10** 155–168.
Lerner J. & Knobloch, E. 1988 The long-wave instability of a defect in a uniform parallel shear. *J. Fluid Mech.* **189** 117-134.
Lin, C. C. (1961) Some mathematical problems in the stability of parallel flows. *J. Fluid Mech.* **10** 430–438.
A. Manfroi & Young, W. R. (2002) Stability of $\beta$–plane Kolmogorov flow. *Physica D* **162** 208—232.
Maslowe, S. A. (1981) Shear flow instabilities and transition. In *Hydrodynamics Instabilities and the transition to turbulence*, eds. Swinney, H. L. & Gollub, J. P., Springer, Berlin.
Orr, W. M. F. (1907) The stability or instability of the steady motions of a perfect liquid and of a viscous liquid. *Proc. Irish Acad.* A **27** 9–68 and 69–138.
Stewartson, K. (1978). The evolution of the critical layer of a Rossby wave. *Geophys. Astrophys. Fluid Dyn.* **9** 185–200.
Willis, A. P., Peixinho, J., Kerswell, R. R. & Mullin, T. (2008) Experimental and theoretical progress in pipe flow transition. *Phil. Trans. R. Soc.* A **366** 2671–2684.

**URLS**

Figure 1:
`https://publicaffairs.llnl.gov/news/news_releases/2007/images/bluegene_sim_colors_349x349s.jpg`
`http://www.math.ubc.ca/~njb/Research/spectra.htm`
`http://www.efluids.com/efluids/gallery/gallery_pages/JH003/text.jsp`
`http://www-frd.fsl.noaa.gov/mab/scatcat/`
`http://www.i-cool.org/?p=124`

Figure 2: `http://www.flometrics.com/products/fluids_lab/reynold1_transition2.jpg`.

# Chapter 2

# Vortex axisymmetrization

## 2.1 Introduction

The study of the instability of vortices goes back to Rayleigh (1880) and to Kelvin (1880). The former derived his celebrated criterion to examine axisymmetric instability. The latter looked at the instability of what would today be called a vortex patch. The neutral modes that he found are called Kelvin waves (not to be confused with Kelvin waves in oceanography – oceanographers and meteorologists call waves on a vorticity gradient Rossby waves).

More recent work has examined the problem of axisymmetrization: does a perturbed vortex return to axisymmetry? There is a subtlety: it is the streamfunction that becomes axisymmetric. The non-axisymmetrical structure in vorticity winds up in a spiral, and the coarse-graining effect of the inverse Laplacian operator acting on the vorticity leads to algebraic decay in time of the streamfunction (Bassom & Gilbert 1998). Figure 2.1 shows examples of vortices that do not and do return to axisymmetry, respectively, for the same disturbance amplitude.

It is clear that some vortices cannot return to axisymmetry. As mentioned before, vortices with compact support in space may support neutral Kelvin modes and hence cannot return to axisymmetry. Dritschel (1998) carried out contour dynamics simulations that exhibited these undamped disturbances in the nonlinear regime.

Experiments with non-neutral plasmas (Driscoll & Fine 1990) and rotating fluids (van Heijst, Kloosterziel & Williams 1991) have examined finite-amplitude perturbations to axisymmetrical vortices. The resulting nonlinear evolution is not predicted by linear theory. In plasma physics, the decay of the streamfunction has an analogue in the Landau damping of the electric field. It is generally accepted that perturbations of sufficient amplitude do not decay back to the undisturbed state, but instead excite a finite-amplitude wave, known in plasma physics as a BGK-mode (Bernstein, Greene & Kruskal 1958).

We develop a defect theory that examines the fate of the Kelvin mode of the compact smooth approximant as the latter becomes an extended structure. It becomes a *quasi-mode*, i.e. (in linear theory) a solution of the initial-value problem whose streamfunction decays exponentially while the vorticity wraps up. Our approach is based on the defect theory of Chapter 1. The small parameter measures the difference between approximants

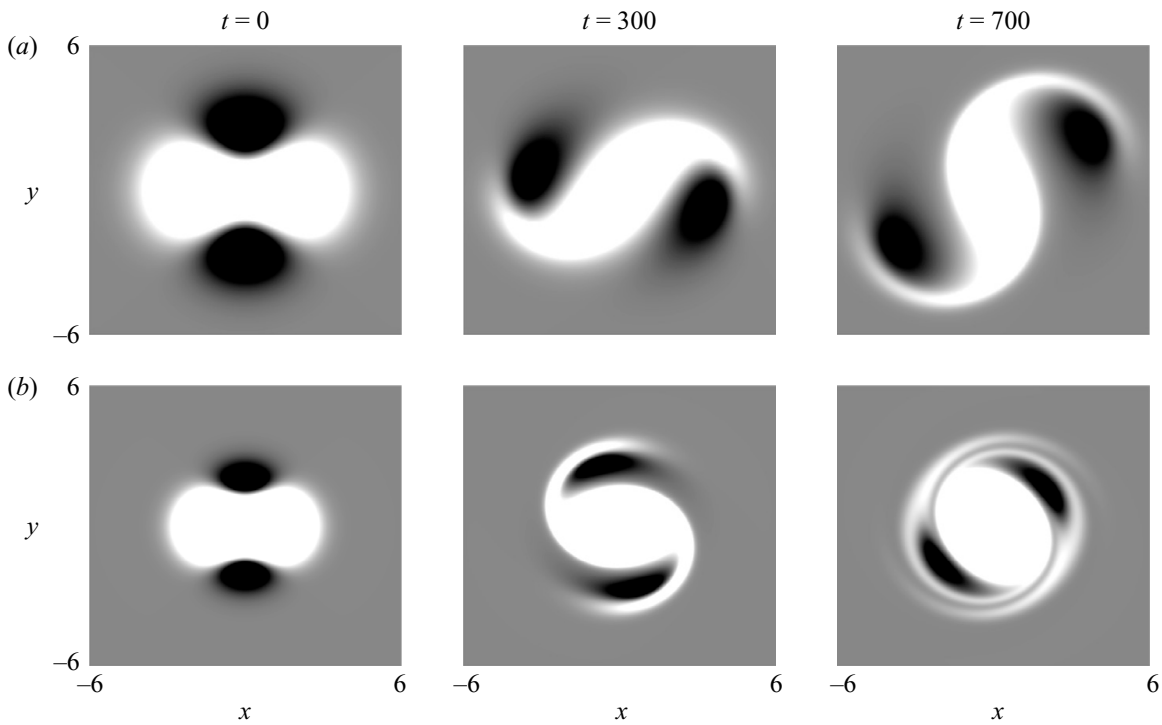


Figure 2.1: Evolution of Gaussian and tanh vortices with superimposed mode 2 disturbance. From Turner & Gilbert (2008).

and the Gaussian vortex. Details may be found in Balmforth, Llewellyn Smith & Young (2001). Examples of subsequent work are Le Dizès and Laporte (2002) and Turner & Gilbert (2008).

## 2.2 Stability of two-dimensional vortices

First a brief digression on linear stability theory for plane vortices, i.e. flows with azimuthal velocity $u_\theta(r)$. Rayleigh's equation has a near-identical form to the plane parallel case (Chapter 1) and one can obtain an analog of Rayleigh's theorem stating that if the basic-state vorticity is monotonic, the vortex is stable. Rayleigh's determinant is a different quantity that concerns only axisymmetric flows.

Part of the motivation for understanding the stability of vortices comes from their prevalence in simulations of two-dimensional turbulence. Gent & McWilliams (1984) provide a careful review of linear stability calculations for axisymmetric vortices.

## 2.3 Defect formulation

### 2.3.1 Setup

In ideal fluid theory, any circular vortex is a possible equilibrium; we consider only stable vortices. In polar coordinates $(r, \theta)$, the Euler equation governing perturbations to such a basic state with angular velocity $\Omega(r)$ and vorticity $Z(r)$ is

$$r\zeta_t + \Omega r\zeta_\theta - (\psi_\theta + \psi_\theta^{\text{ext}})Z' + \frac{\partial(\psi + \psi^{\text{ext}}, \zeta)}{\partial(r, \theta)} = 0. \tag{2.1}$$

The disturbance vorticity $\zeta$ and the disturbance streamfunction $\psi$ are related by

$$\zeta = \psi_{rr} + r^{-1}\psi_r + r^{-2}\psi_{\theta\theta}, \tag{2.2}$$

where $\psi^{\text{ext}}(x, y, t)$ is an externally imposed, irrotational streamfunction which models the perturbing influence of distant vortices or boundary conditions.

We consider 'compact vortices', for which $Z(r) = 0$ if $r > R_{\text{C}}$. We can approach the Gaussian vortex more and more closely by varying a parameter $p$ say. Sometimes these vortices have Kelvin modes, which are the solution to the eigenproblem for $\omega_m$,

$$(\Omega_{\text{C}} - \omega_m)rg = Z'_{\text{C}}f. \tag{2.3}$$

Compact vortices may avoid the critical-level singularity if $r_m > R_{\text{C}}$ because $Z'_{\text{C}}(r_m) = 0$.

We add small, non-compact, axisymmetric vorticity perturbation to a compact vortex, creating a dynamically important critical layer at $r_m$. The new profile is

$$Z(r) = Z_{\text{C}}(r) + \epsilon Z_{\text{S}}(r), \qquad \Omega(r) = \Omega_{\text{C}}(r) + \epsilon\Omega_{\text{S}}(r), \tag{2.4}$$

and $\epsilon$ is defined so that

$$\max_r Z_{\text{S}}(r) = Z_{\max}, \qquad \text{(definition of } \epsilon). \tag{2.5}$$

Figure 2.2 shows that the Gaussian vorticity profile, $Z_{\text{G}} = Z_{\max}\exp(-r^2/{R_{\text{G}}}^2)$, can be represented as the sum of a dominant compact vortex and a smaller 'skirt'. Specifically, in figure 2.2, where $p = 0$ through 5, one has $\epsilon = 0.366, 0.135, 0.057$, and so on. Note that we cannot make the error arbitrarily small: the perturbation scheme that underlies our analysis is founded on the existence of a Kelvin wave to leading order and these cease to exist for large enough $p$.

### 2.3.2 The expansion

We limit ourselves to a compact vortex with an $m = 2$ Kelvin mode at a critical radius at $r = r_2$. We insert (2.4) into (2.1) with the additional scaling assumptions

$$[\psi(r, \theta, t), \zeta(r, \theta, t)] \to \epsilon^2[\psi(r, \vartheta, \tau), \zeta(r, \vartheta, \tau)] \qquad \psi^{\text{ext}}(r, \theta, t) \to \epsilon^3\psi^{\text{ext}}(r, \vartheta, \tau). \tag{2.6}$$

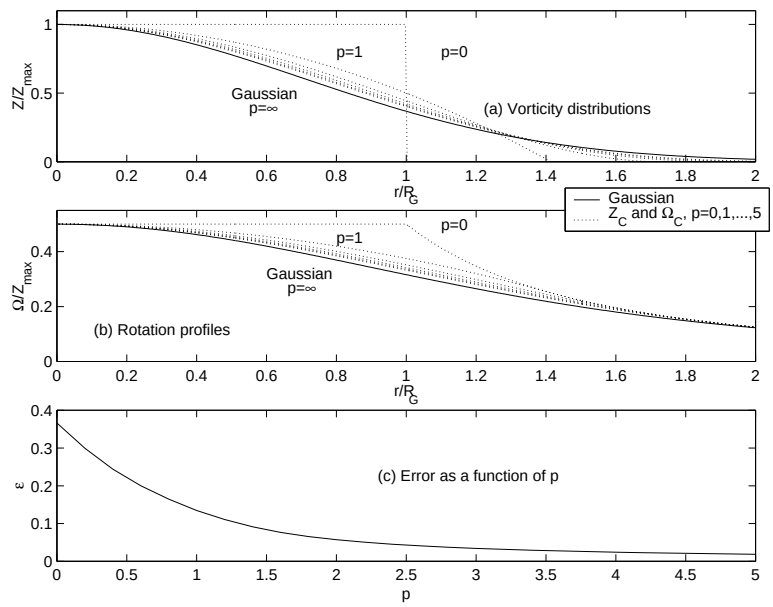


Figure 2.2: The family of compact vortices that approximate the Gaussian vortex, showing scaled vorticity, scaled angular velocity and the small parameter $\epsilon$ as a function of $p$.

These scalings ensure that the response of the system to leading order is a quasi-mode that evolves linearly outside the defect region. In (2.6) we have also changed frame so that the coordinate system is corotating with the speed of the compact vortex at $r_2$:

$$\vartheta \equiv \theta - \omega_2 t, \qquad \tau = \epsilon t \tag{2.7}$$

so that the variables now depend only on the slow time $\tau$. The scaling assumptions in (2.6) and (2.7) also ensure that the nonlinear terms appear at the same order as the external forcing. The scaled equations of motion are

$$\epsilon r \zeta_\tau + (\tilde{\Omega}_\mathrm{C} + \epsilon \Omega_\mathrm{S}) r \zeta_\vartheta - \left(\psi_\vartheta + \epsilon \psi_\vartheta^{\mathrm{ext}}\right)\left(Z_\mathrm{C}' + \epsilon Z_\mathrm{S}'\right) + \epsilon^2 \frac{\partial(\psi + \epsilon\psi^{\mathrm{ext}}, \zeta)}{\partial(r, \vartheta)} = 0. \tag{2.8}$$

In (2.8), $\tilde{\Omega}_\mathrm{C}(r) \equiv \Omega_\mathrm{C}(r) - \Omega_\mathrm{C}(r_2)$ is, to leading order, the rotation rate in new frame. We assume that the external perturbation has the irrotational form

$$\psi^{\mathrm{ext}} = r^2 \left[\hat{b}(\tau) e^{2\mathrm{i}\vartheta} + \hat{b}^*(\tau) e^{-2\mathrm{i}\vartheta}\right] \tag{2.9}$$

and expand $[\psi, \zeta]$.

The leading-order outer equation is

$$\tilde{\Omega}_\mathrm{C} r \zeta_\vartheta^0 = Z_\mathrm{C}' \psi_\vartheta^0, \tag{2.10}$$

with the solution

$$\left[\psi^0, \zeta^0\right] = a\left[f, g\right], \qquad a(\vartheta, \tau) \equiv \hat{a}(\tau) \mathrm{e}^{2\mathrm{i}\vartheta} + \hat{a}^*(\tau) \mathrm{e}^{-2\mathrm{i}\vartheta}. \tag{2.11}$$

In (2.11), $\hat{a}(\tau)$ is the amplitude of the Kelvin eigenmode of the compact vortex $Z_C$. With the normalization $f(r_2) = 1$, $\psi^0(r_2, \vartheta, \tau) = a(\vartheta, \tau)$.

To determine $\hat{a}(\tau)$, we follow the usual path of asymptotics: proceed to higher order with the aim of enforcing a solvability condition on the next-order corrections. This has two effects: solvability ensures that the asymptotic ordering of the solution remains intact, and the solvability condition, the Fredholm Alternative, provides the evolution equation for $\hat{a}(\tau)$. In the present case, however, there are some subtleties in the theory that significantly enrich the asymptotic description. These originate completely as a result of critical-radius singularity. We now skip a lot of detail and just present the result. The critical element is the first-order $m = 2$ mode of the streamfunction, which can be shown to be

$$\psi_2^1(r, \vartheta, \tau) \approx \psi_2^1(r_2, \vartheta, \tau) + \mu_2(r - r_2) \ln|r - r_2|\hat{a} + (r - r_2) \begin{cases} c^- & \text{if } r < r_2, \\ c^+ & \text{if } r > r_2, \end{cases} + \cdots. \quad (2.12)$$

Then the equation for $\hat{a}$ becomes

$$\mathrm{i}\mathcal{I}_1 \hat{a}_\tau + (\mathcal{I}_2 + \mathcal{I}_3 + \mathcal{I}_4)\, \hat{a} = \mathcal{I}_5 \hat{b} + \left(c^+ - c^-\right), \quad (2.13)$$

where the $\mathcal{I}$ are explicit integrals, with $\mathcal{I}_1 > 0$. The goal is now to find an expression for the jump, $c^+ - c^-$, in (2.13). To this end we turn to an analysis of the critical layer at $r_2$.

### 2.3.3 The critical layer at $r_2$

In the inner region, an appropriate radial variable is

$$Y \equiv \epsilon^{-1}(r - r_2). \quad (2.14)$$

The expansion of the streamfunction is

$$\begin{aligned} \psi \;=\; & \psi^0(r_2, \vartheta, \tau) + \epsilon[\psi^1(r_2, \vartheta, \tau) + Y\psi_r^0(r_2, \vartheta, \tau)] + \epsilon^2 \ln\epsilon\, \mu_2 Y \psi^0(r_2, \vartheta, \tau) \\ & + \epsilon^2[\phi + \tfrac{1}{2}Y^2\psi^0(r_2, \vartheta, \tau)] + \cdots. \end{aligned} \quad (2.15)$$

In (2.15), matching to the outer solution has been secured up to and including the terms of order $\epsilon^2 \ln\epsilon$. Matching the terms of order $\epsilon^2$ requires consideration of $\phi(Y, \vartheta, \tau)$.

From (2.15), the leading term in the expansion of the critical layer vorticity is

$$\zeta = \phi_{YY} + \cdots. \quad (2.16)$$

Noting that $Z_C(r_2) = 0$, the leading-order terms from the vorticity equation (2.8) are

$$\phi_{YY\tau} + \left[\Omega_S(r_2) + Y\tilde{\Omega}_C'(r_2)\right] \phi_{\vartheta YY} - r_2^{-1} a_\vartheta \phi_{YYY} = r_2^{-1} Z_S'(r_2) a_\vartheta, \quad (2.17)$$

where $a(\vartheta, \tau) = \psi^0(r_2, \vartheta, \tau)$ is defined in (3.8).

When $|Y|$ is large, the dominant balance in (2.17) is between the right-hand side and the term proportional to $Y$ on the left. Thus

$$\phi_{YY} \sim \frac{\mu_2 a}{Y}, \qquad \text{as } |Y| \to \infty. \quad (2.18)$$

The result above shows that $\phi_{YY}$ matches the second radial derivative of $\psi_2^1$ in (2.12).

The jump $c^+ - c^-$ is now obtained from the critical layer expansion as

$$c^+ - c^- = \lim_{Y^\pm \to \pm\infty} \left[ \int_{Y^-}^{Y^+} \oint e^{-2\mathrm{i}\vartheta} \phi_{YY} \frac{\mathrm{d}\vartheta \mathrm{d}Y}{2\pi} - \mu_2 \hat{a} \ln \left| \frac{Y^+}{Y^-} \right| \right]. \tag{2.19}$$

Here, $Y^\pm = (r^\pm - r_2)/\epsilon$ represent coordinates in the matching regions where $|r - r_c|$ becomes small (but not smaller than $\epsilon$) and $|Y|$ becomes large (though not as large as $1/\epsilon$). But, in the asymptotic theory, we may further take the limit $\epsilon \to 0$, and then replace the limits of the integral in (2.19) by $\pm\infty$.

### 2.3.4 Summary

We now have a closed system of equations: the amplitude of the Kelvin mode, $\hat{a}(\tau)$, is determined by solving the ordinary differential equation (2.13). But the right-hand side of (2.13) involves the jump $c^+ - c^-$, which must be calculated by solving the critical layer vorticity equation (2.17), and evaluating the principal part integral in (2.19). The radial advection in the critical layer vorticity equation is due solely to the velocity field of the mode (these are the terms involving $a_\vartheta$ in (2.17)). The azimuthal advection in (2.17) results from the velocity of the main vortex, $\tilde{\Omega}_\mathrm{C}(r) + \epsilon\Omega_\mathrm{S}(r)$; this term appears as the Taylor-expanded form $\Omega_\mathrm{S}(r_2) + Y\tilde{\Omega}'_\mathrm{C}(r_2)$.

By rescaling space and time scales, we can express the streamfunction as

$$\psi \equiv -(y^2/2) + \varphi(\theta, t), \qquad \varphi(\theta, t) \equiv \hat{\varphi}(t)\mathrm{e}^{2\mathrm{i}\theta} + \hat{\varphi}^*(t)\mathrm{e}^{-2\mathrm{i}\theta}, \tag{2.20}$$

and the vorticity advection equation (2.17) becomes

$$\zeta_t + \frac{\partial(\psi, \zeta + \beta y)}{\partial(\theta, y)} = \zeta_t + y\zeta_\theta + \varphi_\theta \zeta_y + \beta\varphi_\theta = 0. \tag{2.21}$$

The evolution of $\hat{\varphi}(t)$ is then

$$\mathrm{i}\hat{\varphi}_t = \chi + \langle \mathrm{e}^{-2\mathrm{i}\theta}\zeta \rangle, \qquad \text{where } \langle \cdots \rangle \text{ is} \qquad \langle f \rangle \equiv \fint \mathrm{d}y \oint \frac{\mathrm{d}\theta}{2\pi} f(\theta, y, t). \tag{2.22}$$

The principal value integral in (2.22) is necessary because $\zeta \propto y^{-1}$ as $|y| \to \infty$, but we will drop the notation $\mathcal{P}$ from now on.

It is remarkable that the system in this form contains no parameters, except for $\beta = \pm 1$ and those which occur in the specification of the external forcing, $\chi(t)$. If $\beta = -1$ the skirt has increasing vorticity as a function of $r$ and consequently the Kelvin mode is destabilized. Our main concern is the stable case, $\beta = +1$.

We can show using symmetry properties of the model that $\chi$ can be taken to be real without loss of generality. Also we can write $\check{\varphi} = \mathrm{i}\hat{\varphi}$, giving the real equation

$$\zeta_t + y\zeta_\theta + 4\check{\varphi}\cos 2\theta(\beta + \zeta_y) = 0 \qquad \text{and} \qquad \check{\varphi}_t = \chi(t) + \langle \zeta \cos 2\theta \rangle. \tag{2.23}$$

We select two sample forcings:

$$\chi = A\chi_1 = \frac{1}{T^2} At \exp(-t^2/2T^2), \qquad \chi = A\chi_2 = \frac{1}{T^2} At \exp(-t/T). \tag{2.24}$$

In the limit $T \to 0$, both functions amount to an instantaneous kick.

## 2.4 The weakly forced limit: A $\ll$ 1

The amplitude is given by the strength of the forcing. We can construct solutions perturbatively by focusing on relatively small forcing amplitudes. At leading order, we obtain linear dynamics and connect the 'modes' of the skirted vortex to the related non-decaying eigenmode of a compact vortex. Disturbances of finite amplitude do not completely decay, but leave behind 'remnants' that can act as sources of secondary instability (we do not discuss the secondary instabilities).

The linear versions of the amplitude equations (2.21) and (2.22), namely

$$\zeta_t + y\zeta_\theta + \beta\varphi_\theta = 0, \qquad \mathrm{i}\hat{\varphi}_t = \chi + \langle \mathrm{e}^{-2\mathrm{i}\theta}\zeta\rangle, \tag{2.25}$$

can be solved in closed form. For the dynamically active harmonic and zero initial conditions, we obtain

$$\hat{\varphi}_t + \pi\beta\hat{\varphi} = -\mathrm{i}\chi, \tag{2.26}$$

an ordinary differential equation.

If $\beta = -1$, then the homogeneous solution to (2.26) grow exponentially. In this instance, the vortex is unstable and the Kelvin wave of the compact vortex is modified into an unstable mode. However, our interest is in stable vortices with $\beta = 1$ and henceforth we shall focus exclusively on this case.

With $\beta = +1$, the homogeneous solution of (2.26), $\hat{\varphi} \propto \exp(-\pi t)$, provides the simplest example of hydrodynamic Landau damping. That is, the streamfunction decays exponentially while the accompanying vorticity is sheared out to ever smaller scales without decaying in amplitude. The exponential decay of $\hat{\varphi}$ results from spatial averaging (the $\langle\rangle$ in (2.25*a*)). This does not correspond however to a discrete, decaying mode. The vorticity is evidently not separable in $y$ and $t$. It always remains order one, but becomes increasingly sheared. This is why we refer to the disturbance on the non-compact vortex as a Kelvin quasi-mode.

By contrast, Bassom & Gilbert (1998) found that Gaussian vortices have streamfunctions that decay algebraically along the pathway to axisymmetrization. There are terms that lie at higher order in our inner expansion that do, in fact, lead to a protracted algebraic decay at large times.

The damping of the Kelvin quasi-mode becomes arbitrarily small as the vortex is made more compact. Essentially, this observation allows us to reconcile the apparent difference between truly compact vortices and smooth, almost compact vortices. Whereas the latter do not have true discrete modes, they have quasi-modes with very low damping rates. As a result, these modes can appear much like the true modes of compact vortices. Ultimately, however, the quasi-mode wraps up the residual vorticity gradient inside the critical layer and must decay.

Though we have considered only inviscid vortices, it is relevant at this juncture to mention a property of the viscous problem. Specifically, with the introduction of viscosity the Landau damped quasi-modes can be transformed into true eigenmodes (Balmforth 1998). Thus the Kelvin quasi-mode may become a real eigenmode when a small amount of viscosity is present.

When we disturb the vortex, the induced perturbation does not completely decay away, but leaves a mean remnant that is itself unstable if the initial forcing amplitude is high enough. Thus, we cannot expect that the vortex always axisymmetrizes. In fact, if kicked hard enough, the vortex should suffer secondary instability and develop non-axisymmetrical structure;

## 2.5 The strongly forced limit: A $\gg$ 1

We consider the impulsive case by taking $T \to 0$ in the forcing functions so that $\chi(t) = A\delta(t)$. We introduce a small parameter $\varepsilon$ defined by $\varepsilon \equiv \frac{1}{\sqrt{2A}}$. In the limit $\varepsilon \to 0$ the dynamics can be reduced to a passive scalar advection problem. Notice that in order not to violate our original scaling assumptions $A$ cannot be as large as $\epsilon^{-1}$. Consequently $\varepsilon$ must be greater than $\sqrt{\epsilon}$.

Rescaling appropriately and adopting a perturbation expansion in $\varepsilon \ll 1$ shows that the leading order vorticity, $q \equiv y + \zeta_0$, is obtained by solving a passive scalar advection equation

$$q_t + yq_\theta + 2q_y \cos 2\theta = 0. \tag{2.27}$$

This passive scalar problem is discussed by O'Neil (1965), Stewartson (1978), Warn & Warn (1978) and Killworth & McIntyre (1985) in related contexts.

A perturbative calculation shows that as $t \to \infty$ the streamfunction is $\breve{\varphi}(\infty) = (1/2) - 1.543\varepsilon + O(\varepsilon^2)$. This shows that nonlinearity prevents a perturbed vortex from relaxing back to axisymmetry.

As $t \to \infty$ the vorticity becomes crenellated in $y$. The amplitude of these wiggles remains finite but their scale is increasingly fine as $t \to \infty$. A coarse-grained average filters the oscillations and reveals a nontrivial structured averaged field. Because of symmetry this averaged vorticity is zero within the cat's eye (that is, within the area where $\psi > -1$). Outside the cat's eye, the averaged vorticity takes a nonzero mean value which can be calculated. We determine that coarse-grain average by arguing that advection cannot transfer any vorticity through the steady streamlines and consequently the amount of vorticity contained within the differential area enclosed by two adjacent streamlines (a streamtube) is constant. Thus the coarse-grained average is obtained by taking the initial vorticity pattern, $q(\xi, y, 0) = y$, and making an average over a streamtube. Following Rhines & Young (1983), this streamtube average is

$$\bar{q}(\psi) = \oint y \frac{\mathrm{d}\ell_\psi}{|\nabla\psi|} \Big/ \oint \frac{\mathrm{d}\ell_\psi}{|\nabla\psi|}, \tag{2.28}$$

where $\ell_\psi$ is the arclength around a streamline. It is clear from the symmetry of the initial condition that $\bar{q}(\psi) = 0$ within the region of closed streamlines where $\psi > -1$. Outside the cat's eye, where $\psi < -1$, the streamtube average is nonzero, and can be calculated by converting the contour integrals in (2.28) to integrals with respect to $\xi$.

## 2.6 Numerical solutions

We now turn to the full nonlinear problem for arbitrary forcing and solve the equations numerically. The integration scheme is an operator splitting scheme based on the algorithm of Cheng & Knorr (1976).

### 2.6.1 Weak forcing

By 'low-amplitude', here, we mean simulations that appear to show axisymmetrization ($\breve{\varphi} \to 0$ as $t \to \infty$). As indicated above, such behaviour can only be expected for values of the forcing amplitude $A$ below some threshold depending on $T$.

In Figure 2.3 we show streamfunction amplitude as functions of time for both $\chi = A\chi_1$ and $\chi = A\chi_2$. The solutions all show an initial evolution that follows the linear theory. But beyond a certain time, the Landau damping is interrupted by a slower decay. Note that the low-amplitude oscillations in figure 2.3 that become visible at about $t = 4$ arise due to the finite domain in which the system is numerically solved (see Appendix A). These are spurious, as can be seen by changing the domain size which changes their amplitude and period.

As predicted by the asymptotic theories of section 4, the streamfunction decays provided $A < A_c(T)$; that is, the vortex axisymmetrizes. If $A > A_c(T)$, the streamfunction enters a different behavioural regime in which $\varphi$ undergoes large-amplitude oscillations. These 'bounces' coincide with the initial turning over of a cat's eye. A physical rationale for the threshold is that there are two characteristic timescales in the problem (excluding $T$): the time for Landau damping and the characteristic turn-over time in the core of the cat's eye. Broadly speaking, if the damping time greatly exceeds the turn-over time, we may expect that cat's eyes form without much decay of the streamfunction. However, if the damping time is much shorter than the turn-over time, a cat's eye cannot complete even one bounce before it disappears. Hence, there should be an amplitude threshold if the two effects are competitive.

### 2.6.2 Formation of cat's eyes

When $A > A_c$, we unambiguously observe the creation of cat's eye structures. A typical example is shown in Figure 2.4 for $\chi = A\chi_2$ with $T = 1$. Qualitatively, the visual appearance of the cat's eyes is not sensitive to $A$ and $T$, nor to the type of forcing function, provided $A$ well exceeds the critical threshold. This remains true even when the forcing function decays less quickly than the natural Landau damping.

Runs with different values of $A$ show that for small $A$ the streamfunction amplitudes follow the linear solution over relatively long initial times. For larger $A$, the solution departs from the linear case almost immediately. In each case, the decay of the streamfunction halts and $\hat{\varphi}(t)$ begins to oscillate. The inception of these oscillations corresponds to the initiation of circulation in the core of the cat's eye. There are two main differences between cases with low and high $A$. The first is that the crenellation of $\zeta$ is far more significant in lower amplitude solutions. The result is that the cat's eye has a more complicated structure in its early stages of development (and is consequently more prone to

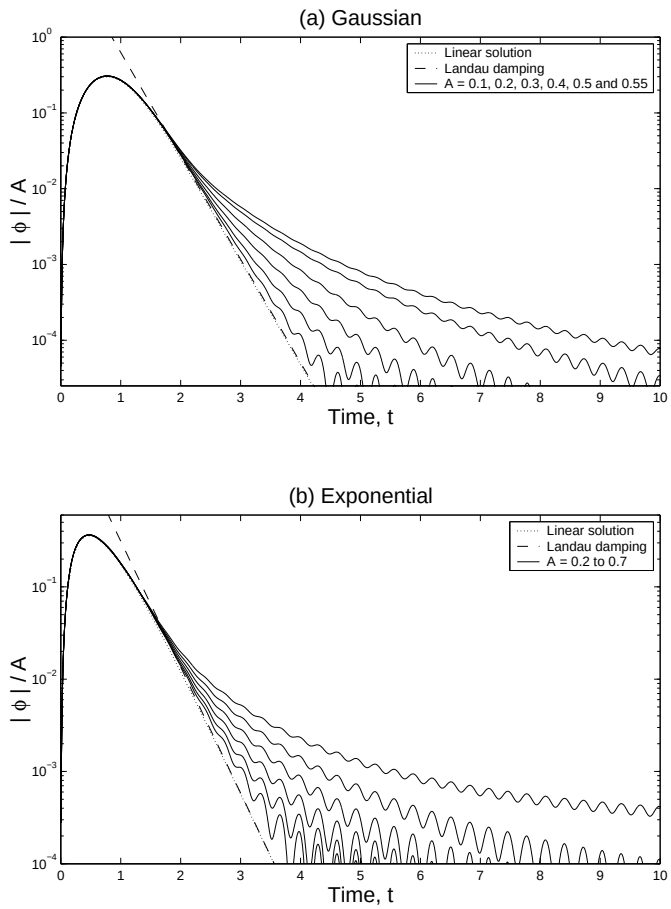


Figure 2.3: Scaled streamfunction amplitudes, $|\check{\varphi}(t)|/A$, against time for (a) $\chi = A\chi_1$ and $T = 0.5$, and (b) $\chi = A\chi_2$ and $T = 0.2$. In each case, results for different forcing amplitudes, $A$, are shown, The linear result is also shown together with the trend of Landau damping.

numerical error). The second difference concerns the streamfunction. For small $A$, $\check{\varphi}(t)$ passes repeatedly through zero. This means that the vortex core overturns one way for a while, but then unwinds for a subsequent interval. Overall, it is not clear whether the core ultimately creates a cat's eye, or whether the vorticity simply continues to wind and unwind. In other words, the asymptotic state may be time dependent.

### 2.6.3 Coarse-grained steady states

Both the numerical results and the strongly forced problem illustrate the importance of finite-amplitude steady states. These states are described by the time-independent version of our model system, which implies that $q = y + \zeta$ is any function of the total streamfunction, $\psi = -y^2/2 + 2\check{\varphi}\cos 2\theta$. That is, $\zeta + y = q(\psi)$. This function need only satisfy the consistency condition, $\langle e^{-2i\theta} q(\psi)\rangle = 0$, which does not greatly constrain the possibilities.

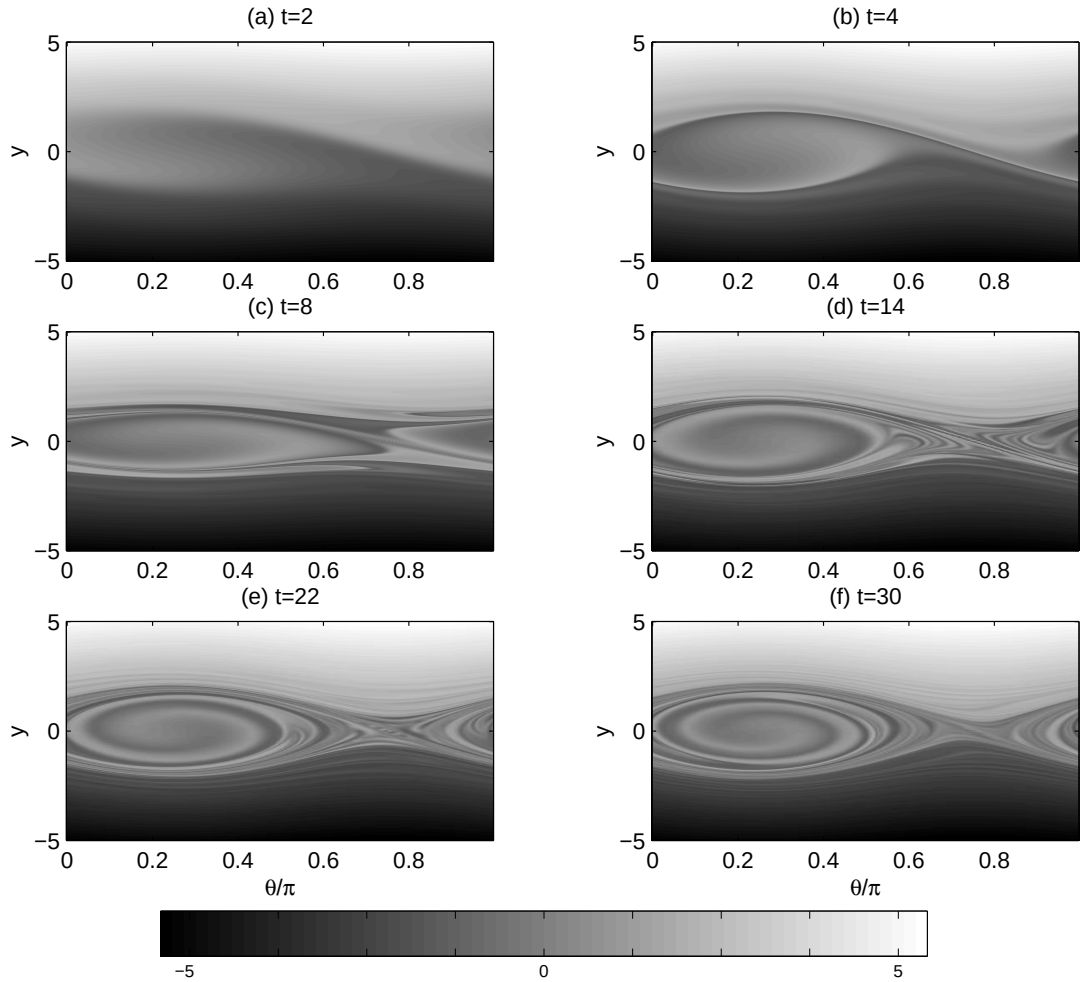


Figure 2.4: A solution with $\chi = 2.72\chi_2$ with $T = 1$. Shown is a grey-scale map of the total vorticity, $y + \zeta$, at the times indicated.

The initial condition used in the computations has $\psi = -q^2/2$. This relation is rapidly lost in the initial evolution. But over long times, there is evidence that the numerical solutions converge to states with another $q$-$\psi$ relation. This is illustrated in Figure 2.5, which shows a snapshot at $t = 40$ of a solution computed for the $\chi = 2.5\chi_1(t)$ case with $T = 1$. At this time, the vorticity has been wrapped into a fairly tight spiral inside the cat's eye, and the outer vorticity field is completely sheared out (the numerical integration has smoothed over much of this structure). However, the plot of $q = \zeta + y$ against $\psi$ shows two populations of points. The first population lies outside and near the separatrix of the cat's eye (see panel ($c$)).

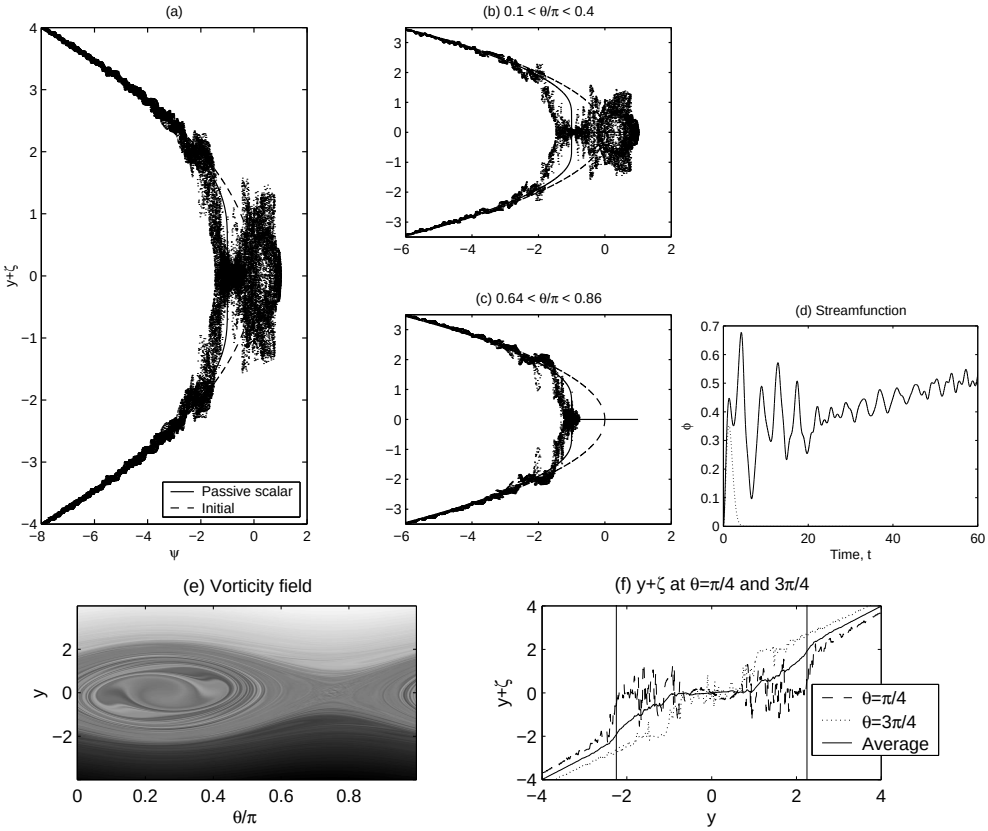


Figure 2.5: (*a*) Plots of $\psi$ against $y + \zeta$ for $\chi = 2.5\chi_1(t)$ with $T = 1$, at time $t = 40$. In (*b*), we plot $\psi$-$q$ points only for the region with $0.1 < \theta/\pi < 0.39$, which corresponds to a section encompassing the centre of the cat's eye. Panel (*c*) is a similar picture for $0.66 < \theta/\pi < 0.86$, which contains the hyperbolic point of the separatrices. Also plotted in panels (*a*)–(*c*) are the $q$-$\psi$ relations for the initial condition (the dotted parabola) and the passive scalar solution, which is the solid curve. The solid-passive-scalar curve consists of two branches. Panels (*d*)–(*f*) display some further features of the corresponding solution.

## 2.7 Conclusions

Our asymptotic analysis takes advantage of the fact that nearly compact, stable vortices have a special sensitivity to external perturbations. Specifically, the scaling of the external perturbation is taken to be order $\epsilon^3$, yet the response of the quasi-mode is order $\epsilon^2$. This is a kind of resonance, and requires that the external forcing has frequency content matching the rotation frequency of the quasi-mode. The linear solution is summarized schematically in the formula

$$\psi = \epsilon^2 \,(\text{exponentially decaying quasi-mode}) + \epsilon^3 \,(\text{algebraically decaying contributions})\,, \tag{2.29}$$

as in Chapter 1. In linear theory axisymmetrization occurs in almost all circumstances.

The effect of nonlinearity is to slow the decay of the quasi-mode, or even arrest that

decay if the initial amplitude of excitation exceeds a threshold. Above the threshold, cat's eye structures form, and, in the case of an $m = 2$ perturbation, the result is a tripolar vortex, as seen in experiments. Because the forcing is scaled to be order $\epsilon^3$, this threshold is actually small. Thus, finite-amplitude cat's eyes are the generic outcome of resonantly exciting the quasi-mode of the vortex.

We expect that the reduced model (2.20)–(2.22) is broadly applicable as a model of linear and weakly nonlinear relaxation in ideal plasmas and fluid shear flows. In analogy with plasma physics, one might call this system the 'single-wave model'.

## 2.8 References

### Articles


Balmforth, N. J., Llewellyn Smith, S. G. & Young, W. R. (2001) Disturbing vortices. *J. Fluid Mech.* **426** 95–133.

Bassom, A. P. & Gilbert, A. D. (1998) The spiral wind-up of vorticity in an inviscid planar vortex. *J. Fluid Mech.* **371** 109–140.

Bernstein, I. B., Greene, J. M. & Kruskal, M. D. (1958) Exact nonlinear plasma oscillations. *Phys. Rev.* **108**, 546–550.

Cheng, C. Z. & Knorr, G. (1976) The integration of the Vlasov equation in configuration space. *J. Comp. Phys.* **22**, 330–351.

Driscoll, C. F. & Fine, K. S. (1990) Experiments on vortex dynamics in pure electron plasma. *Phys. Fluids B* **2** 1359–1366.

Dritschel, D. G. (1998) On the persistence of non-axisymmetric vortices in inviscid two-dimensional flows. *J. Fluid Mech.* **371** 141–155.

Gent, P. R. & McWilliams, J. C. The instability of barotropic circular vortices. *Geophys. Astrophys. Fluid Dyn.* **35** 209–233.

Killworth, P. D. & McIntyre, M. E. 1985 Do Rossby-wave critical layers absorb, reflect or over-reflect? *J. Fluid Mech.* **161** 449–492.

Le Dizès, S. & Laporte, F. (2002) Theoretical predictions for the elliptical instability in a two-vortex flow. *J. Fluid Mech.* **471** 169–201.

O'Neil, T. M. (1965) Collisionless damping of nonlinear plasma oscillations. *Phys. Fluids* **8** 2255–2262.

Turner, M. A. & Gilbert, A. D. (2008) Thresholds for the formation of satellites in two-dimensional vortices. *J. Fluid Mech.* **614** 381–405.

van Heijst, G. J. F., Kloosterziel, R. C. & Williams, C. W. M. (1991) Laboratory experiments on the tripolar vortex in a rotating fluid. *J. Fluid Mech.* **225** 301–331.

Warn, T. & Warn, H. (1978) The evolution of a nonlinear critical level. *Stud. Appl. Maths* **59** 37–71.